



Acoustic preliminary design of a low-noise fan stage considering a variable-area nozzle and variable-pitch rotor blades

A. Moreau¹ · R. Schnell¹ · M. Mennicken¹

Received: 19 December 2022 / Revised: 23 March 2023 / Accepted: 27 March 2023
© The Author(s) 2023

Abstract

A low-noise low-pressure ultra-high-bypass-ratio fan stage to be implemented in the next generation of aircraft engines is described and evaluated acoustically with semi-empirical and analytical methods suited for preliminary design. As expected, good reduction potentials are observed for the jet noise and fan tonal noise components when the UHBR design is compared to current fans in service. However, concerns are identified for fan broadband noise, which are attributed to the off-design operation of the UHBR fan too close from its stability limit. By unloading the fan and thus reducing the size of the rotor wakes, the variable-area nozzle provides a substantial fan broadband noise reduction with a nozzle opened by around 15% from its design value. Alternatively, with the variable-pitch fan, closing the rotor blades by roughly 5° turns out to be an even more effective method to reduce fan noise, as the unloading mechanism is combined with a stronger tilting of the rotor wakes and a lower intra-stage flow Mach number. Opening the nozzle or closing the blades beyond the setting that provides the best fan efficiency is not recommended as the acoustic benefit progressively vanishes, whereas technical feasibility becomes more challenging. Finally, the presence of one of these systems may allow for the design of a low-solidity rotor, with a smaller contribution from the rotor wakes and thus a weaker fan noise emission.

Keywords Fan noise · Semi-empirical and analytical prediction · UHBR engine · Variable-area nozzle · Variable-pitch fan

Abbreviations

A/C	Aircraft
UHBR	Ultra-high bypass ratio
DP	Aerodynamic design point (cruise)
SL	Acoustic point take-off sideline
AP	Acoustic point approach
VAN	Variable-area nozzle
VPF	Variable-pitch fan
GTF	Geared turbofan
FPR	Fan pressure ratio
SM	Surge margin
OGV	Outlet guide vanes, stator
OAPWL	Overall sound power level rel. to 10 ⁻¹² W
TON	Tonal noise
BBN	Broadband noise

List of symbols

Q	Mass flow in kg/s
N	Rotation speed in rpm

D_{fan}	Fan diameter at rotor entry in m
M	Flow Mach number
M_{tr}	Rotor tip relative Mach number
A_{wake}	Non-dimensional area of the rotor wakes
ψ	Stage work coefficient
B/V	Rotor blade count/OGV (stator) count
ΔA	Relative opening of nozzle area in %
$\Delta \chi$	Variation of blade pitch angle in deg
$\Delta \sigma$	Relative variation of rotor solidity in

1 Introduction

1.1 Motivation

As part of its strategy for sustainable aviation, the German Aerospace Center (DLR) is currently developing a novel “middle-of-the-market” aircraft concept specifically aimed for low-noise emission. This work is carried out within the research project SIAM (“Schallimmissionsarmes Mittelstreck-enflugzeug”). A substantial component of that effort is made up by the preliminary design of an ultra-high-bypass-ratio (UHBR) turbofan engine whose fan stage targets a pressure ratio around 1.3 in Cruise flight conditions. This corresponds

✉ A. Moreau
Antoine.Moreau@dlr.de

¹ DLR, Institute of Propulsion Technology, Cologne, Germany

to an engine bypass ratio of 16, which is situated at the upper end of the reasonable range for ducted turbofans. Low-pressure-ratio fans are known to improve the specific fuel consumption and to generate less jet noise and fan tonal noise; however, they operate closer to their aerodynamic-stability limit at off-design and part-speed conditions. As a result, considering variable-geometry systems, such as a variable-area fan nozzle (VAN) or variable-pitch fan blades (VPF), is mandatory during the preliminary design process. As we will see in this study, there are also substantial acoustic benefits to be expected from these systems.

1.2 State of the art

The variable-area nozzle has been so far mostly examined from the point of view of engine thermodynamic cycle, e.g., Giannakakis [2] and Kyritsis [9], its mechanical implementation with Sain [17], and fan aerodynamic performance by Kavvalos [7]. Kavvalos estimated that significant surge margin improvements by 20–25% can be realized with a nozzle opening by 20% from its nominal area (around 4–5% gain per 1% opening). A few studies were dedicated to the acoustic assessment of that technology: Michel [13] estimated the impact on jet noise with a benefit of 2 dB with 15% opening; Woodward [23] observed from the NASA SDT fan noise tests a reduction of 2 dB overall sound power noise, with reductions in fan broadband noise by 3 and 5 dB with an area opening of 5% and 11%, respectively. Also, a reduction of the fan interaction tones was observed. A more recent study published by Moreau [16] has extended the scope of Michel's theoretical evaluation to the acoustic impact of the VAN on fan noise. A parametric study realized on fan stages with varying design pressure ratio showed that fan broadband noise emission is very significantly improved with a VAN, and that the gain is especially large for low-pressure-ratio fans.

The variable-pitch fan blades also have received mostly attention in terms of fan aerodynamic design. Joksimovic [5] evaluated the required pitch variations to maintain a 10% surge margin over a complete mission, with pitch angles around ± 2 deg. Williams and Hall [22] considered this technology from the perspective of reverse-thrust generation applied to the low-pressure NASA ADP fan. Kavvalos [7] estimated that a pitch change of +8 deg at take-off improves the surge margin by 33% (which means a 4–5% gain per degree). As for the VAN technology, the acoustic impact of the VPF has not been yet extensively documented. To the authors' knowledge, the only publications on that topic were provided by NASA in the 1970s. Glaser [4] reported on experiments of a very-low-pressure fan (with FPR = 1.20) with a VPF for short-take-off and landing aircraft application, with the objective to enable reverse thrust but also as a way to optimize thrust-noise relations. He found out that

the rotor pitch angle has a measurable impact on noise and that the aerodynamically optimal pitch is the one related with the lowest noise emissions. In parallel, Lown (1977) [10] published a study on tests with VPF for the design of a wind-tunnel drive.

1.3 Objectives of the study

The present study is a continuation of the authors' work [16] previously dedicated solely to the variable-area nozzle at efficiency-optimal nozzle opening. Here, the objective is first to assess the acoustic impact of that technology on the UHBR fan stage designed specifically for the low-noise aircraft of the SIAM research project. Variations of the nozzle area beyond the efficiency-optimal nozzle opening are also considered for potential further noise reduction. The second objective is to include the other technology, the VPF, and to compare its impact with that of the VAN within the same modelling framework. The working principles on how each of this technology provides a noise reduction are also highlighted. A third objective is to evaluate how the implementation of the variable-geometry systems may in turn affect the design of the fan and may thus further reduce noise at the source.

2 Methodology and implementation of variable geometry

2.1 Fan pre-design and aerodynamic/acoustic evaluation

A global and simplified modelling approach, described in details by Moreau [14], is adopted to fulfill the objectives of the present study. It is also this approach that was followed in the previous study by the author dedicated to the VAN in 2021. The method consists of an integrated multi-disciplinary thermodynamic/aerodynamic/acoustic framework based on semi-analytical models (in-house tool PropNoise), which was developed and validated in the past with the purpose of rapidly and robustly assessing different fan designs in terms of acoustic emission.

As shown in Fig. 1 in the S2 axial-radial plane, the engine is simplified by considering only a single stream without modelling the core engine. Resolving separately the core flow would make the approach much more complex without affecting noticeably the noise emission from the fan dominant sources and the jet. Therefore, the engine is solely constituted of an intake duct and a rotor–stator fan stage equipped with a nozzle at the exhaust. Moreover, the thermodynamic and aerodynamic aspects of the problem are addressed with a meanline approach, whereas acoustic emission is calculated from radially extrapolated flow

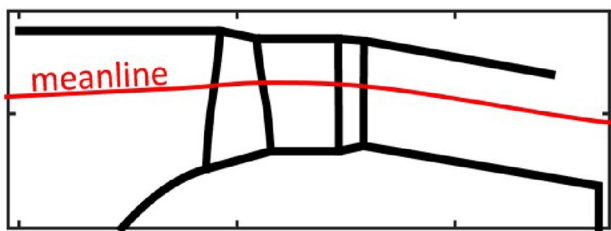


Fig. 1 Simplified engine model with meanline approach

distributions, thus following a strip approach. The representative meanline radius is located at 70% of the duct channel height, where most of the aerodynamic work is performed.

Figure 2 represents schematically the procedure that is carried out for each of the configurations of interest. The first step of the procedure is the engine sizing, where the fan diameter is scaled, such that the required thrust in Cruise flight is delivered with a value of 36 kN at 10,500 m altitude, which is typical for a civil mid-range aircraft of the A320 class. Also, during this step, the design of the fan blades is performed: the metal angles of the rotor blades and stator vanes at their respective leading and trailing edges are optimized, such that they maximize the fan efficiency at the specified rotation speed, N , and mass flow, Q , under the constraint of a fan pressure ratio, FPR, also known and specified at the design point (typically mid-cruise).

Once the geometry parameters necessary for off-design calculations have been determined and fixed, the second step of the procedure is to calculate the aerodynamic performance map of the fan and to determine the position of the acoustic certification points within that map by specifying the thrust to be delivered by the engine and the atmospheric pressure at which the nozzle exhaust flow should expand—choked conditions at the nozzle exit are captured by the model, but in practice, they occur only in cruise (DP) for engines with a pressure ratio above 1.35. The acoustic points considered in this study are take-off sideline (SL) and approach (AP), and take-off cutback is ignored owing to its relative proximity

with sideline. Thrust values of 160 kN and 40 kN at altitudes 120 m and 0 m are assumed, respectively, for the A320-class aircraft considered here.

With the position of SL and AP established in the fan map, all acoustic-relevant off-design flow parameters, such as flow Mach numbers and rotor blade wake size, can be calculated and passed to the acoustic module. No acoustic treatment is implemented in the intake and exhaust duct sections. Jet noise is estimated with the single-stream model developed by Stone [21]. The tonal and broadband components of the rotor–stator interaction are the sources calculated for fan noise estimation, according to Goldstein’s version of the linear Acoustic Analogy as implemented by Moreau [14]. For high-speed fans, the tonal rotor self-noise (also known as buzz-saw noise) is calculated with a non-linear approach [15].

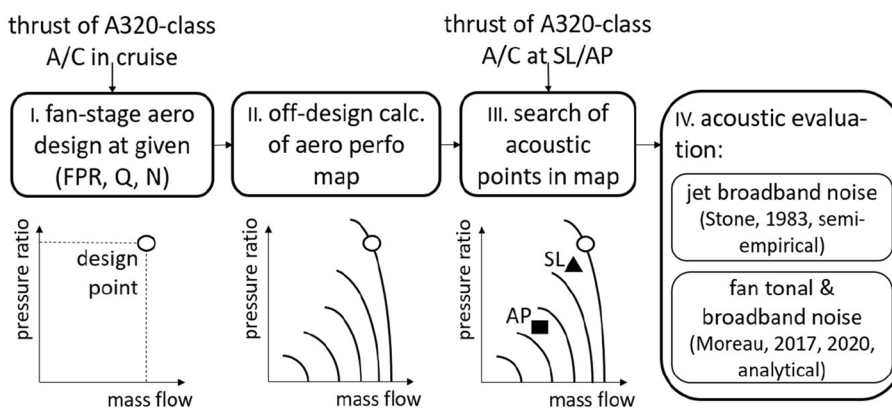
Some details are given now about the physical modelling underlying the estimation of fan noise. The analytical model by Moreau [14] for rotor–stator noise interaction provides a sound power that basically scales with flow quantities inside the fan stage. Equation (1) shows that sound power scales with some power (around 5) of the flow Mach number M between rotor and stator, and with the square of the velocity perturbation related to the rotor wakes, represented by a wake area A_{wake}

$$OAPWL \sim 10 \log_{10}(D_{fan}^2 \cdot M^5 \cdot A_{wake}^2) + \text{const.} \tag{1}$$

Another approach, based on empirical correlations by NASA [8], relies only on global performance parameters such as the mass flow Q and the total-temperature rise across the rotor ΔT_t , as described in Eq. (2). The exponent on ΔT_t was increased from 2 in the original correlations to 4 in Krejsa to account for a stronger and more realistic sensitivity of noise on the throttling effect, which is related to incidence variations; this is also discussed later on, in Sects. 4.1 and 4.2

$$OAPWL \sim 10 \log_{10}(Q \cdot \Delta T_t^4) + \text{const.} \tag{2}$$

Fig. 2 Procedure to evaluate the acoustic emission for each fan configuration of interest



Because the approach of Eq. (2) does not resolve the impact of the variable-geometry systems at the level of velocity triangles and intra-stage flow—as presented in the Sects. 2.2 and 2.3—it may not capture some of the acoustic trends as we will see when comparing the predictions provided by both methods (1) and (2) later in chapter 4.

Coming back to the approach by Moreau [14], the wake area introduced in Eq. (1) is first estimated at the meanline radius using the following relation of Eq. (3):

$$A_{\text{wake}} = \delta^* / h = \omega_{\text{visc}} / 2 / \left(1 + M_{\text{rel,in}}^2 / 2 \right). \quad (3)$$

The wake area is defined as the non-dimensional ratio of the blade boundary-layer displacement thickness δ^* to the flow passage height h , which is equivalent to a flow blockage factor. It is calculated with the viscous loss coefficient of the rotor blades and inflow Mach number. This relation was developed and validated recently [11] on a fan stage similar to the reference GTF design considered in the present study. The aerodynamic loss coefficient ω is also evaluated at the meanline and calculated with Eq. (4) from an inviscid shock-bound contribution and the viscous contribution from the boundary layer, which results from skin friction over the rotor wetted surface and from the boundary-layer thickening near the leading edge of thin slender blades under incidence, such as those of a high-subsonic/transonic rotor, as described by Freeman and Cumpsty [1]. Shock loss and leading-edge loss are computed with their model, to which the friction loss is added to obtain the total loss of Eq. (4)

$$\omega = \omega_{\text{shock}} + \omega_{\text{visc}}, \quad \text{with} \quad \omega_{\text{visc}} = \omega_{\text{BL,LE}} + \omega_{\text{BL,fric}}. \quad (4)$$

The component $\omega_{\text{BL, fric}}$ of the viscous loss basically scales with the solidity of the rotor blades (product of blade count \times chord length), whereas the component $\omega_{\text{BL, LE}}$ depends primarily on aerodynamic loading and the rotor incidence angle. That separation of the loss components and the sensitivity of broadband noise to the wake area has been recently investigated by Meier zu Ummeln and Moreau [11].

Finally, a brief description of the method implemented for the estimation of the stability margin, or surge margin, of the fan is given. One of the usual candidates for surge margin definition is chosen here and given in Eq. (5)

$$\text{SM} = 1 - \text{FPR} / \text{FPR}^{\text{surge}} \cdot Q^{\text{surge}} / Q|_{N=\text{const}}. \quad (5)$$

In that equation, the performance pair (FPR, Q) is evaluated along an iso-rotation-speed line and compared to the pair at the surge point ($\text{FPR}^{\text{surge}}$, Q^{surge}). The definition of the surge point is subject to controversy, and many versions exist without one being well established, but all are related to some loading criterion. Here, we consider that stability is ensured as long as enough axial thrust is generated by the stage: the surge point is defined as the point on the speed

line where the axial thrust of the stage has decreased by just 20% of its maximum value along the speed line, which is by experience a rather tolerant criterion. Therefore, the absolute values of surge margin are likely to be over-optimistic; however, its relative variations are expected to be reasonably predicted. It should also be noted that Kavvalos [7] worked with a different definition of surge margin, $\text{SM} = (\text{FPR}^{\text{surge}} - \text{FPR}) / (\text{FPR}^{\text{surge}} - \text{FPR}^{\text{min}})|_{Q=\text{const}}$, which is more sensitive to variations in FPR owing to the lower value of the denominator, $\text{FPR}^{\text{surge}} - \text{FPR}^{\text{min}}$, compared to that of Eq. (5). Hence, any comparison requires to be cautious.

2.2 Modelling approach for variable-area nozzle

The acoustic impact of the variable-area nozzle is modelled through its effect on the aerodynamic conditions at which the fan operates. During the second step of the calculation procedure detailed in Sect. 2.1, the nozzle area is set to a specified value different from that at the design point—typically, the nozzle is opened by around 15% of its design value. As the nozzle exhaust flow expands at the same atmospheric pressure irrespective of its cross-section area (unchoked nozzle at the acoustic points), opening the nozzle leads to an increase in mass flow and a decrease in pressure ratio for the engine to deliver the same thrust as in the fixed-nozzle configuration. The rotation speed may be either augmented or reduced, depending on the nozzle opening, but this change is limited to less than $\pm 3\%$ and can be neglected in the following qualitative discussions that explain the driving mechanisms.

Figure 3 shows a view in the S1 plane (meridional–circumferential plane) of the rotor blade at the meanline radius. The driving mechanism is the increase in axial velocity, at nearly constant rotation speed. Opening the nozzle thus results in a decrease of the incidence at the rotor blade leading edge, thereby unloading the fan with a smaller wake as a consequence. As demonstrated later in Sect. 4 precisely that effect is responsible for the changes in acoustic emission from the fan. It should be also noted that the absolute velocity at the rotor exit is slightly increased.

As previously analyzed by Moreau [16] and illustrated in Fig. 4, the variable-area nozzle shifts the operating point of the fan away from its surge line by an amount that depends on the opening of the nozzle exhaust area relative to its design value determined at cruise conditions.

2.3 Modelling approach for variable-pitch blades

As for the variable-area nozzle, this system modifies the aerodynamic conditions of the off-design operating points, thus affecting the acoustic emission from the fan. Here, however, the nozzle retains a constant opening, which is that of the design point; the geometric parameter that varies is the

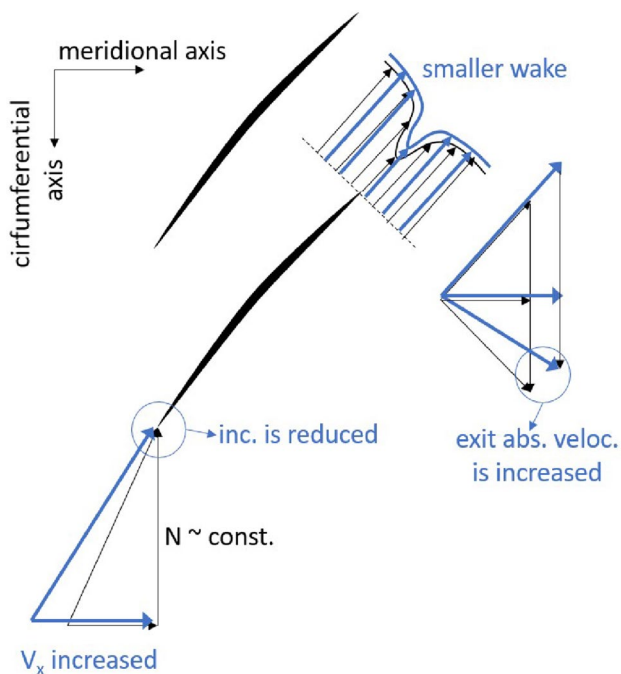


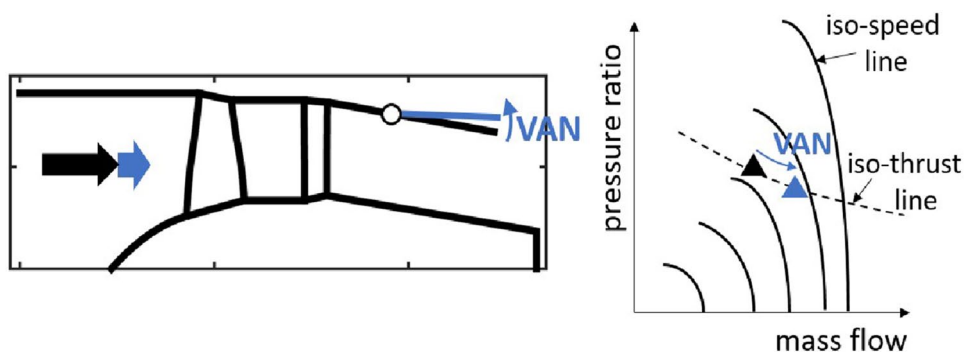
Fig. 3 Impact of variable-area nozzle on the velocity triangles and wake of the rotor

pitch of the rotor blades, or the angle at which the blades are rotated along their own radial axis, and thus staggered relative to the engine axis. The stator vanes pitch setting is kept constant for the sake of mechanical simplicity, because stator vanes are usually designed for a relatively wide range of incidences.

The method to determine how a change in rotor pitch affects the location of the off-design operating points is similar to that used with the variable-area nozzle. However, the search for the new location of the point is performed within the modified fan map, which is structured by steeper iso-speed lines when the rotor blades are closed, and a smaller maximum mass flow achievable on a given iso-speed line.

Figure 5 exemplarily shows how a typical fan map is affected by closing the rotor blades by a few degrees. As

Fig. 4 Impact of variable-area nozzle on the flow through the fan (left) and the shift of off-design operating points within the aerodynamic performance map (right)



the nozzle area is fixed, the mass flow through the fan that corresponds to expansion at atmospheric conditions is also fixed. Therefore, the same fan pressure ratio as without VPF is required to deliver the specified thrust. As a result, the location of the operating point in the (FPR, Q) plane is unchanged; a small shift may be induced during the searching procedure due to variations of fan efficiency; however, this shift can be considered negligible for the range of interest in this study. Also, a small variation in rotation speed (between 0 and 5%) results from the new operating-point search; however, it may be neglected during the upcoming explanations of the driving mechanism.

Figure 6 shows in the S1 meanline plane how closing the blades affects the flow around the rotor: it primarily induces a reduction in incidence angle, thus lowering the aerodynamic loading and yielding a smaller wake. In contrary to the case of the variable-area nozzle, the wake is also more strongly tilted. Moreover, that tilting effect reduces the circumferential component of flow velocity, the swirl, in the absolute reference frame behind the rotor; this is a significant difference compared with the VAN and—as we will see in chapter 4—has implications on fan noise emission.

3 Evaluation of the baseline UHBR fan

3.1 Presentation of the reference fan stages

Before assessing the acoustic impact of the variable-geometry systems on the next-generation UHBR fan, the baseline version of this fan with fixed geometry is presented and compared with state-of-the-art current designs. Overall, three fan stages corresponding to three different generations of engines equipping a mid-range civil aircraft of the A320 class are presented in this section and compared with each other in terms of aerodynamic performance and acoustic emission. Table 1 summarizes the main characteristics of each of the reference fans.

The first generation is represented by the fan of the V2500 engine and has a design pressure ratio around 1.6. This

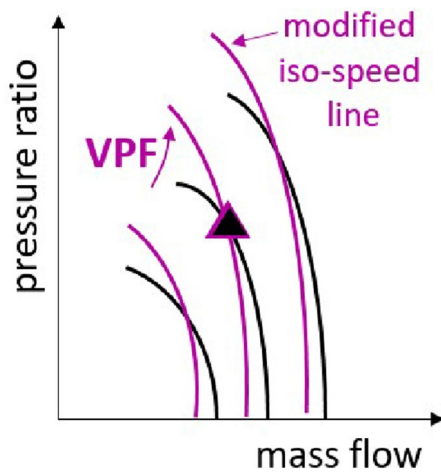


Fig. 5 Impact of the variable-pitch system on the iso-speed lines and on the relative position of the operating point in the fan map

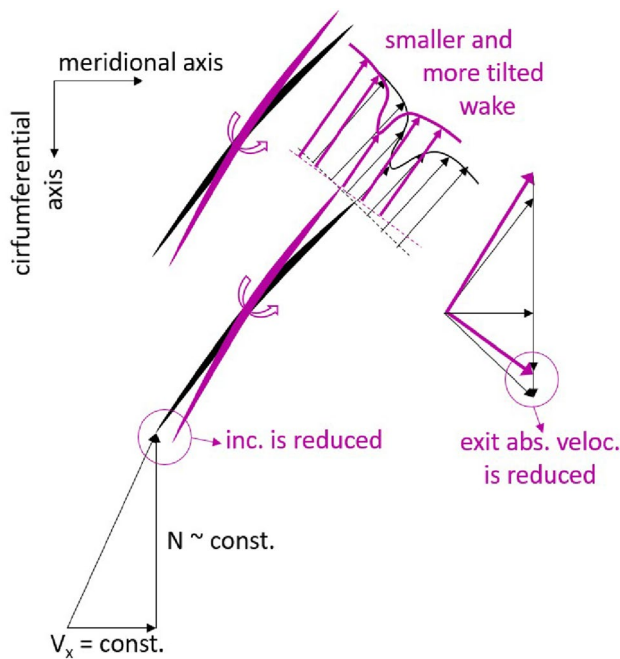


Fig. 6 Impact of variable-pitch rotor blades on the incidence and wake

Table 1 Main design parameters of the reference fans

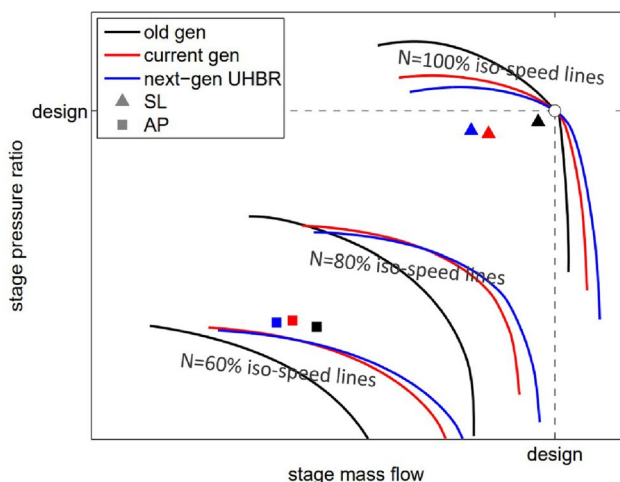
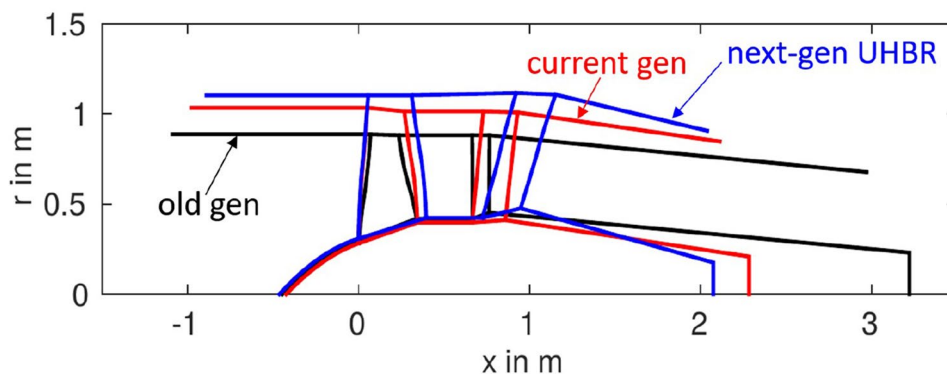
	Old-gen V2500	Current-gen GTF	Next-gen UHBR
D_{fan}	1.61 m	2.05 m	2.24 m
B/V	22/60	22/38	16/36
perfo. @ DP			
FPR	1.6	1.38	1.31
BPR	7.5	12	15.5
M_{tr}	1.46	1.14	1.05
ψ	0.27	0.32	0.32

engine is mounted on the DLR ATRA research aircraft [18, 20]. It operates with a supersonic rotor at take-off conditions. The second generation of fans has a pressure ratio around 1.4 and represents the first generation of geared turbofans (GTF) currently in service, which operate with a low-speed fan near the sonic limit at take-off and are driven by the low-pressure turbine via a gearbox. The fan stage design was developed by Kaplan [6] at DLR. Finally, the next generation of engines currently planned among the industry to enter into service during the next decade is the UHBR fan, with a design pressure ratio near 1.3 and fan speeds below the sonic limit at all acoustic certification points. The fan is also driven by the turbine via a gearbox.

The UHBR baseline fan chosen for implementation in the DLR SIAM project is a combination of two designs recently finalized by the DLR Department of Fans and Compressors. The first one was studied by Schnell [19] as part of the EU-funded project Clean Sky ASPIRE, with a focus on low pressure, low noise, and very short intake. The second fan, called STRIVE, was designed by Mennicken [12] as part of a consortium, led by German–Dutch Wind Tunnels (DNW), formed for the DNW-internal EPS project (electrically powered engine simulator). It is concerned with the design and realization of a fully representative, direct electrically driven UHBR-turbofan engine simulator for wind-tunnel applications. The consortium members are DLR (engine operating point’s definition and UHBR fan stage design), NLR (nacelle design and structural analysis and integration), and DNW (electric drive system, consortium lead and overall project definition). Both designs have the same pressure ratio and 16 rotor blades. The SIAM UHBR variant retains the exact same blade design from the STRIVE fan, but with a modified axial gap between rotor and stator that matches the axial extent of the ASPIRE fan stage from rotor entry plane to stator exit plane. Also, the stator vane count is modified from 38 (STRIVE) to 36 (ASPIRE) by keeping the vane solidity constant. Finally, an aerodynamic sweep of 20 degrees is added in streamwise direction on the stator vanes, which is more pronounced than the 10-degree sweep of the STRIVE and ASPIRE designs. Figure 7 shows a side view in the S2 axial/radial plane of the engines which visualizes the respective diameters and axial extent of each fan.

3.2 Comparison of the fan stages

This section provides a comparison of the three generations of reference fans, still without any variable-geometry system implemented for the next-generation UHBR design. The aerodynamic performance maps of the fans are shown in Fig. 8. The horizontal and vertical axes of the maps are scaled to obtain the design point of each fan at the same position. Three iso-speed lines are drawn for each fan at 60% (slightly below Approach), 80% and 100% (design speed,

Fig. 7 Side view of the reference fans**Fig. 8** Scaled aerodynamic performance maps of the reference fans and relative position of the acoustic points SL/AP

slightly above Take-off Sideline). The acoustic points AP and SL are marked by square and triangle symbols, respectively. As already pointed out by Moreau [16], the acoustic points move closer to the stability limit when the design pressure ratio decreases. Thus, the next-generation UHBR fan operates at aerodynamic unfavorable conditions, which also hamper the acoustic benefit gained from its low-speed design, as we will see.

Figure 9 shows a comparison of the fans at AP and SL for three aerodynamic parameters. On the right side, the rotor relative tip Mach number substantially decays with newer engines, the UHBR fan rotor operating in subsonic conditions at all acoustic points. In the center, the wake size of the rotor blades, defined as the non-dimensional area of the wakes related to the flow passage height, is smaller for the UHBR fan, but not by a large amount. This is attributable to the large positive rotor incidence values observed on the left part of the figure and which is higher for newer fan rotors not equipped with a variable-geometry system.

Figure 10 shows the overall sound power levels of three main acoustic components of the sound field radiated by

the reference engines. The fan tonal noise (abbreviation: fan TON) includes the rotor self-noise due to the rotor-locked potential field and shocks, and the interaction of the rotor wakes with the stator vanes. The broadband component of this interaction, induced by the turbulence fluctuations of the wakes, represents the fan broadband noise (abb. fan BBN). Finally, jet broadband noise is considered (abb. jet BBN).

Jet noise is the component where the next-gen UHBR engine shows the highest reduction potential, owing to the low-speed, low-pressure, and low-jet Mach number design. Also, the reduction in fan tonal noise is very strong, which is here mostly due to the increased axial gap, pronounced sweep angle of the stator vanes, and subsonic fan rotor. For the fan broadband noise component, however, the benefit from the UHBR design is only a few decibels. This limited noise reduction potential was already observed by Moreau [14] and is attributed to the higher work coefficient, ψ , at which modern fans tend to be designed to limit their tip speed, as shown in the last row of Table 1. Another important cause for the relatively high broadband noise levels of the UHBR engine is the unfavorable location of the acoustic points within the aerodynamic map, which is too close to the stability limit. The next section explains how both variable-geometry systems may counter this negative effect and provide substantial acoustic gains.

4 Acoustic benefit of variable-area nozzle and variable-pitch blades

4.1 Variable-area nozzle

The acoustic impact of the variable-area nozzle was already addressed by the author in a recent study [16]; however, only evaluations at the optimal nozzle opening area had been provided, corresponding to the maximal fan efficiency. Now, we propose a continuous variation of the nozzle, starting at the design value (0%, no opening in Cruise) up to an increase by 30% of that value. Although technical feasibility is questionable for the upper end of that range, as mechanical

Fig. 9 Aerodynamic parameters of the reference fans: rotor blade incidence (left), rotor wake size (center), and rotor relative tip Mach number (right)

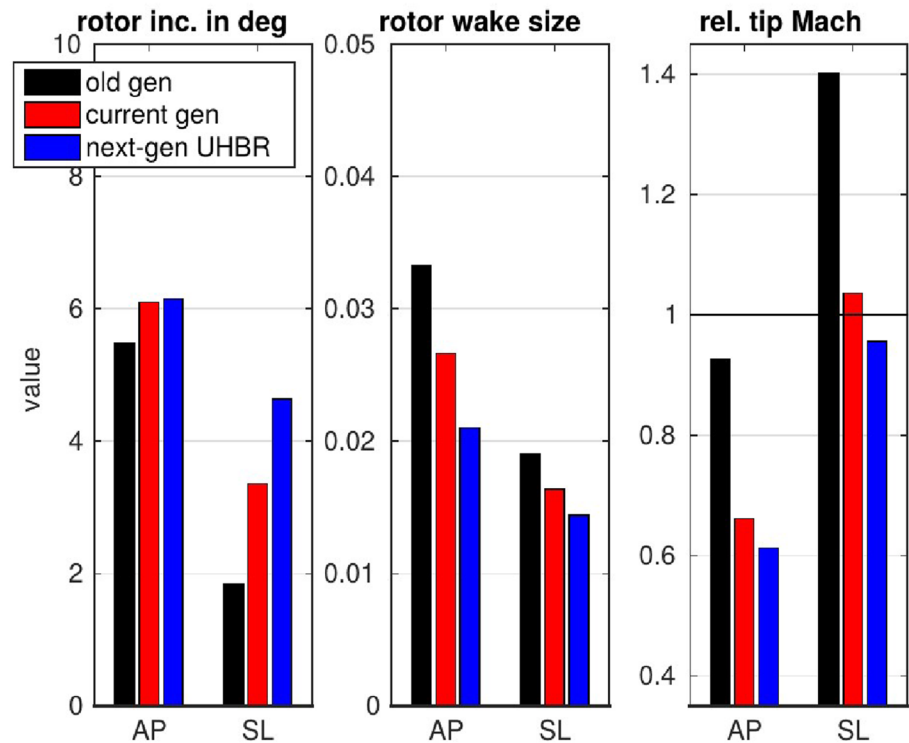
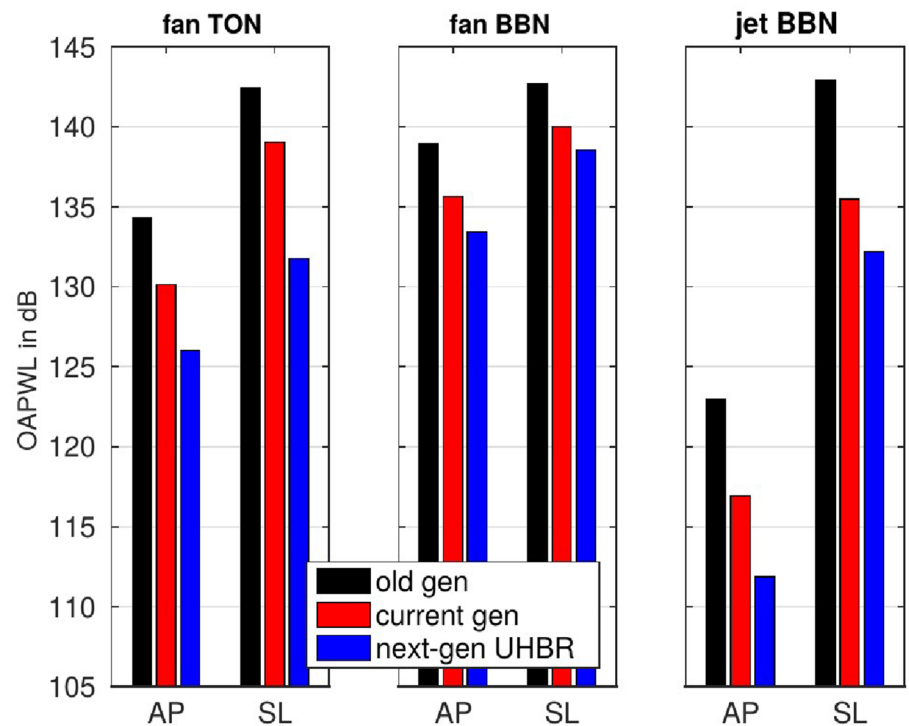


Fig. 10 Overall sound power levels of the reference fans for the three noise components considered: fan tones (left), fan broadband noise (center), and jet noise (right)

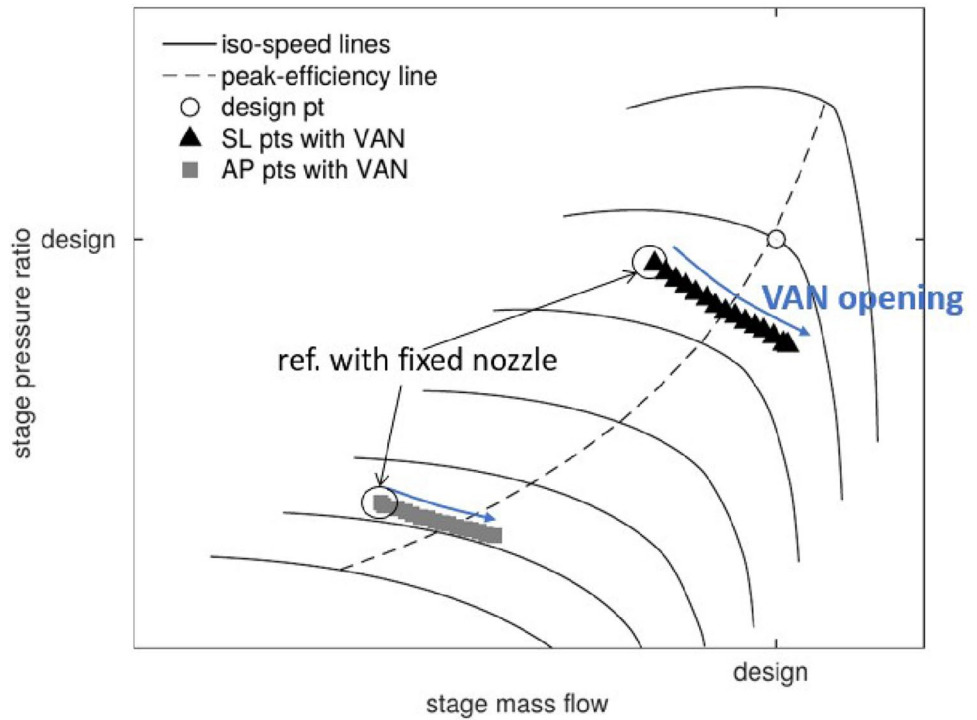


constraints or weight penalties might be prohibitive, the full range is evaluated to determine whether an acoustic optimum exists theoretically.

Figure 11 shows again the aerodynamic performance map of the UHBR fan including the various locations of

the acoustic points AP and SL realized when successively increasing the nozzle area from its design value. The points are distributed along their respective iso-thrust lines and on both sides of the peak-efficiency line. The range of

Fig. 11 Positions of acoustic points within the aerodynamic map of the UHBR fan, obtained by increasingly opening the nozzle



variation thus covers the domain beyond the aerodynamic optimum of the fan.

Figures 12, 13 and 14, show how aerodynamic and acoustic quantities are affected by the nozzle opening, expressed as a relative change of nozzle area ΔA from its value at DP. The black and grey lines depict the evolution of these quantities along the SL and AP iso-thrust lines, respectively. The symbols denote the aerodynamic optimum nozzle opening, where fan efficiency is maximal on each line.

Figure 12 demonstrates quantitatively what the previous fan map figure suggests qualitatively: opening the nozzle shifts the acoustic points away from the stability limit of the fan, thus increasing the stability margin. An increase from 15% up to 30% is predicted with the max opening. This corresponds to a gain of 0.5% per 1% of nozzle opening. This is approximately half the sensitivity found by Kavvalos [7], but he used a different definition of surge margin, more sensitive to variations, as explained earlier in Sect. 2.1. The

Fig. 12 Variation of fan stability (left) and rotor incidence (right) with nozzle opening

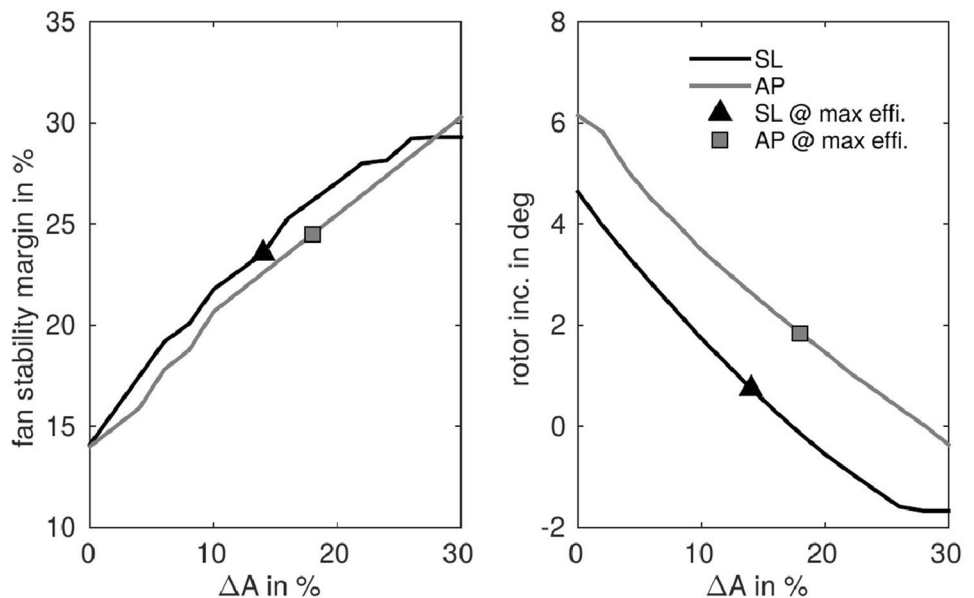


Fig. 13 Variation of fan efficiency, loss/wake area, and flow Mach numbers with nozzle opening

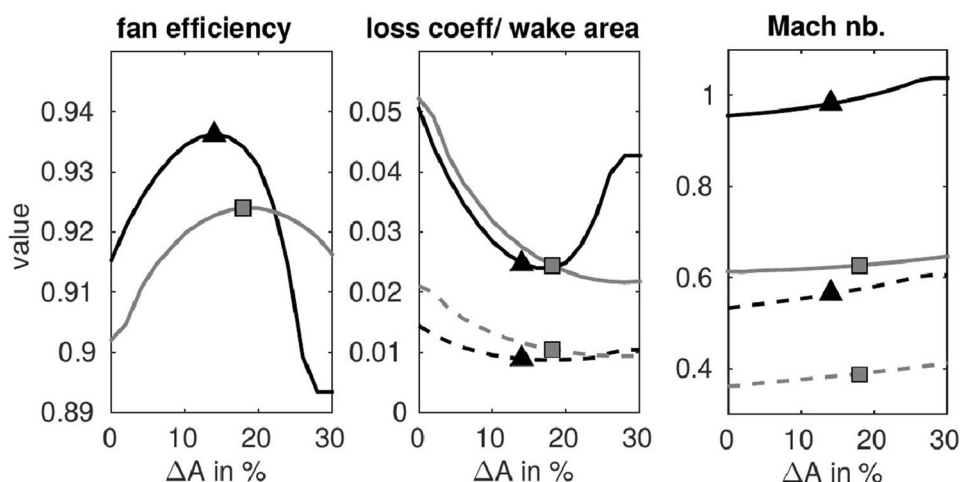
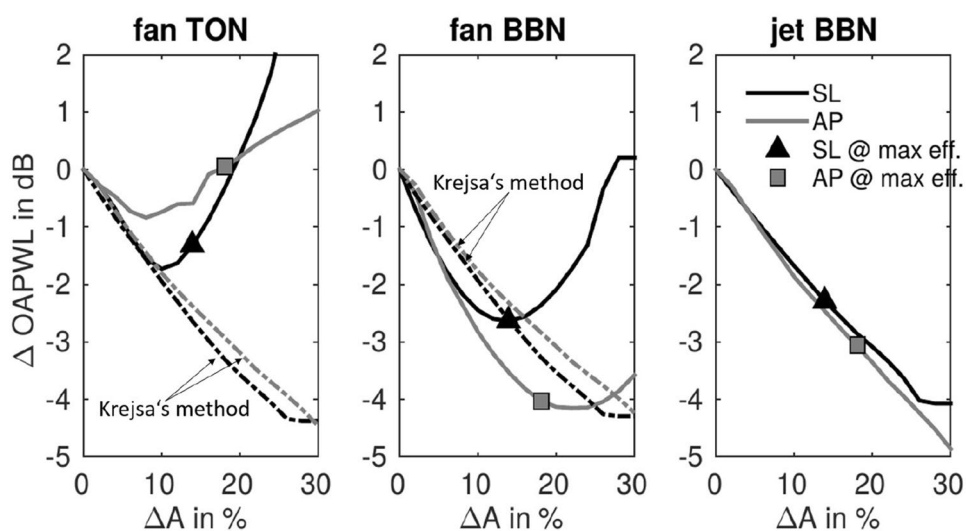


Fig. 14 Impact of nozzle opening on overall sound power of the engine noise components



shift of the acoustic points toward a higher mass flow is also accompanied by a substantial reduction in rotor incidence, leading to zero or even negative incidence for the largest nozzle opening.

Figure 13 presents quantities related to the aerodynamic losses and flow Mach numbers, and follows the same color and symbol code as Fig. 12. On the left, the evolution of fan isentropic efficiency follows as expected a parabolic shape with a maximum corresponding to the aerodynamically optimal nozzle opening. In the center, the loss coefficient of the rotor blades (solid lines) features a similar evolution but with inverted parabolas. The non-dimensional rotor wake area, depicted by the dashed lines, is less sensitive than the aerodynamic loss coefficient to nozzle area variations, especially at the higher fan speeds (SL), but it still decreases with increasing opening before reaching a minimum at opening values slightly above the fan-efficiency-optimal opening. On the right, the flow relative Mach at rotor tip (solid lines) slightly increases when opening the nozzle, which is

mostly due to an increase in axial flow (and to a smaller extent related to the rotation speed variation). The dashed lines depict the Mach number of the flow entering the OGV, thus driving the strength of the rotor–stator wake interaction. This quantity also increases when opening the nozzle, which is schematically explained in Fig. 3.

The evolution of the three acoustic components already introduced when comparing the reference fans are now shown in Fig. 14. On the right, we observe that jet broadband noise is steadily reduced as the nozzle is opened; along a constant-thrust line, the rise in mass flow must be compensated by a reduction in fan pressure ratio, which leads to a lower jet exhaust Mach number and a weaker source of jet noise.

The fan noise components on the left (tonal) and in the middle (broadband) of the figure are predicted with two methods. The solid lines refer to the analytical methods by Moreau [14, 15], where the size of the rotor wakes is resolved and their interaction with the stator vanes

modelled physically. The dashed lines refer to one of the empirical methods developed by NASA [8]; it does not resolve the physical processes responsible for noise generation but are based on an experimental database gained from static engine tests and includes a newer revision that accounts for a more realistic sensitivity of noise to incidence variations compared to earlier versions of the correlations.

The reduction of fan broadband noise is substantial with 2.5 dB at SL and 4 dB at AP (according to the analytical method), when the nozzle is opened at the fan-efficiency optimum. Opening the nozzle beyond this point does not further lower the noise level of that component. Both analytical and empirical methods predict a similar trend up to the optimal point; beyond this, the analytical model captures the growth of the wake size due to negative incidence or proximity to choking, resulting in higher noise levels, which the NASA correlation does not. Fan tonal noise is much less effectively reduced and may even be larger than at design when the nozzle is too widely opened, and this is attributed to the increase in flow Mach numbers already discussed in Fig. 13. The NASA correlation does not resolve the effect of Mach numbers inside the stage and it basically follows the same trend as for the broadband part.

During the previous study by Moreau [16] about the impact of the VAN at optimal nozzle opening, much higher noise reductions were predicted for fan broadband: 12 dB at SL, and 8 dB at AP for the same design fan pressure ratio of 1.3, hence a much larger sensitivity to nozzle area variations. With the last developments of the method as discussed in Sect. 2.1, the wake area, A_{wake} (only boundary-layer related), rather than the total loss coefficient (which also includes the shock loss), is considered a more suited and physically sound parameter to correlate fan noise. As we see from Fig. 13, the wake area is less sensitive than the total loss coefficient and

the gains predicted with this latest method are considered more realistic; this is further discussed in Sect. 4.3.

4.2 Variable-pitch blades

Concerning the second technology, closing the blades of the fan rotor has a similar unloading effect on the fan aerodynamics as opening the nozzle, but, in that case, neither the airflow nor the pressure ratio is changed. There are, however, small departures from that trend, due to variations in fan efficiency but also due to artifacts from the numerical implementation of the operating-point searching procedure. This is visible in Figs. 15, 16, and 17, for the Approach condition (grey lines) at 9° pitch setting: a spike is observed that does not correspond with the physical trend.

Figure 15 shows the variation of fan stability margin and rotor incidence when closing the blades by angles between 0 and 15 degrees. The effect is similar to that of the VAN, but here we observe an improvement of stability from 15% to around 30% with blades closed by 10° , which is equivalent to a gain of 1.5% per degree. This value is smaller than what Kavvalos [7] found out, again, this is attributed to the definition of surge margin he implemented.

In Fig. 16, the rotor efficiency, rotor loss coefficient and wake area, and flow Mach numbers are shown (same color and symbol code as in Fig. 15). We observe an optimum, close to the fan-efficiency optimum, beyond which the size of the wakes grows again. As a result, closing the blade beyond that optimum generates more fan broadband noise as represented in Fig. 17. The abatement of fan tonal and broadband noise is here again very significant with gains up to 6 dB compared with the fixed-pitch reference at Approach conditions. We note that the empirical NASA method predicts a much lower reduction of noise while closing the blades; however, as this method correlates noise with global

Fig. 15 Variation of fan stability (left) and rotor incidence (right) with pitch setting

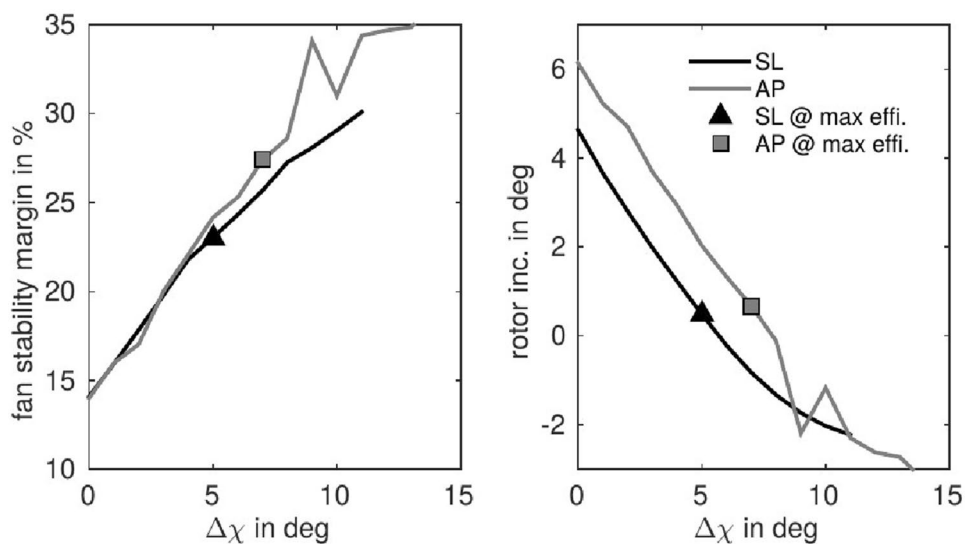


Fig. 16 Variation of fan efficiency (left), loss and wake size (center), and Mach numbers (right) with pitch setting

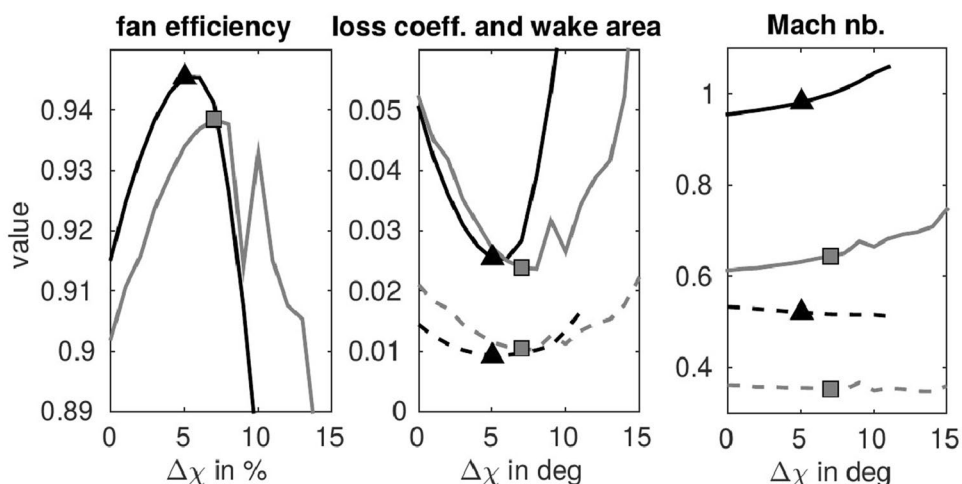
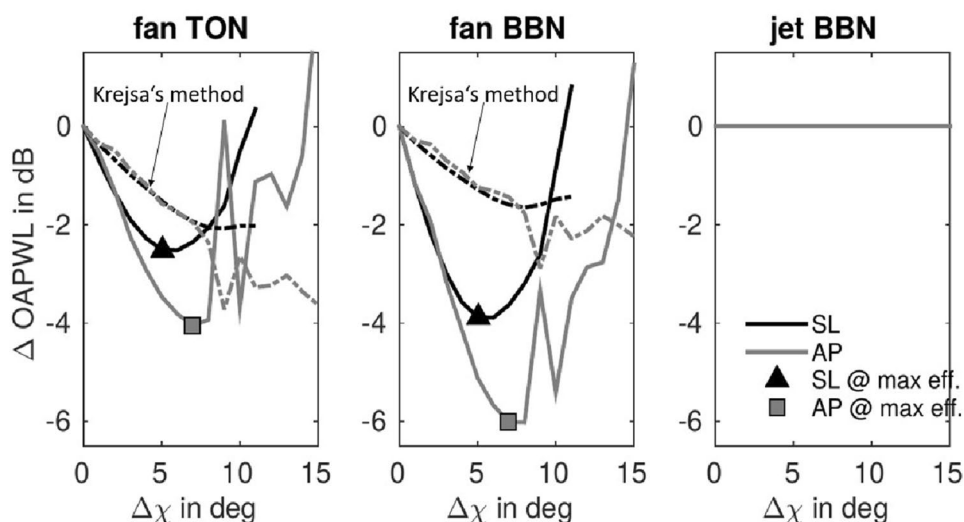


Fig. 17 Impact of pitch setting on overall sound power of the three noise components of interest



fan performance rather in-stage physical quantities like wakes and flow velocities, the sensitivity is much lower than that with the analytical method. As the airflow and pressure ratio remain unchanged by the VPF, the jet Mach number is unaffected and jet noise is not reduced.

It should be observed from the right part of Fig. 16 that the rotor tip relative Mach number (solid lines) increases with increasing pitch setting (this is attributable to the faster rotating rotor); however, the intra-stage Mach number (dashed lines) slightly decreases when the rotor is more strongly staggered. This is one of the differences compared with the variable-area nozzle, and this is detailed in the next section.

4.3 Comparison of the VAN and VPF systems

The aerodynamic performance of both variable-geometry systems is now compared by representing the evolution

of the stability margin and fan efficiency as functions of the rotor incidence on the horizontal axis. In Fig. 18, the curves related to the variable-area nozzle are depicted in blue, those related to the variable-pitch-fan in magenta. The Sideline and Approach conditions are represented by solid and dashed lines, respectively. We observe that the gain in stability margin is almost identical with both systems: SM grows by around 2.5% per degree of incidence reduction, and a gain by approximately 10% SM is achieved at the aerodynamic optimum, compared to the fixed-geometry configuration (value at highest incidence in the plots). Fan isentropic efficiency is also greatly improved by around 2% (+0.02) with the VAN and 3% (+0.03) with the VPF, when comparing optimum with reference.

The acoustic performance of both variable-geometry systems is now compared by representing the evolution of the overall sound power levels of Figs. 14 and 17 as functions of the rotor incidence on the horizontal axis. In Fig. 19, again,

Fig. 18 Compared aerodynamic performance of the VAN and the VPF systems: fan stability margin (left) and fan isentropic efficiency (right)

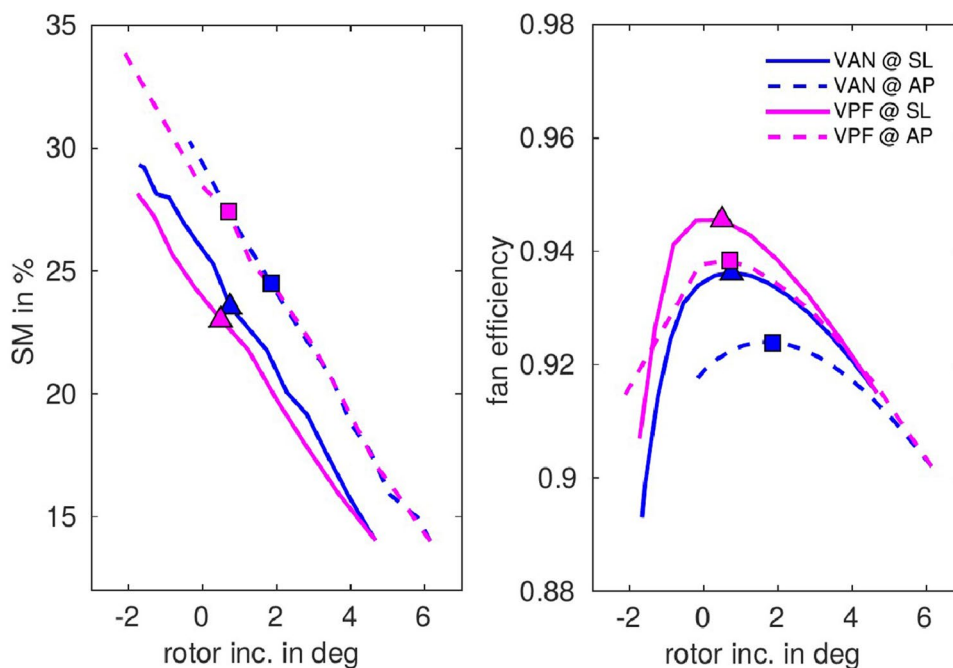
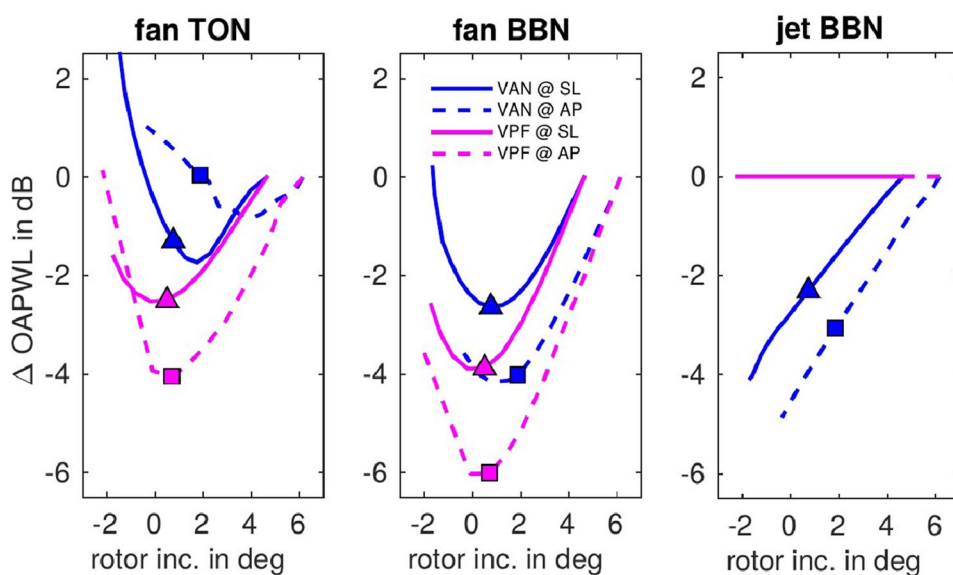


Fig. 19 Compared acoustic performance of the VAN and the VPF systems for the three noise components of interest



the curves related to the variable-area nozzle are depicted in blue, those related to the variable-pitch fan in magenta. We observe that, for the same rotor incidence, the VPF provides a slightly better reduction in fan broadband noise, especially in the optimal region with near-zero incidence. Fan tonal noise is also more effectively reduced by a VPF system. These trends can be explained by the different impact of the VPF on the rotor wake than the VAN: as shown previously in Fig. 6, rotating the blades does not only induces a reduction of incidence; it also tilts the rotor wakes more strongly relative to the engine axis, thus increasing the path over which the wake decays. The reduction in intra-stage

flow velocity, described in Fig. 6 and quantitatively visible in Fig. 16, also explains the stronger benefit from the VPF compared to the VAN.

The only drawback of the VPF compared to the VAN is the absence of jet noise reduction, but this is of secondary importance in a UHBR engine where the overall levels of jet noise are well below those of fan broadband noise, which is the most important source as indicated by Fig. 10.

More generally, the results point out a relatively similar dependence of fan broadband noise to the rotor incidence angle, irrespective of the VAN or the VPF system. A slope of roughly 1.2 dB/deg can be estimated from Fig. 19. It can

be compared with experimental observations from fan tests performed at different throttle positions: Ginder and Newby [3] reported a dependence of fan broadband noise of 1.7 dB/deg in a Mach range of 0.4–0.8. We conclude that the sensitivity predicted by the analytical fan noise model of Moreau [14] based on the wake area (present study) rather than the total loss coefficient [16] is also in line with experimental observations, even though it is apparently slightly underestimated. It suggests, also, that the predicted acoustic gains from the VAN and the VPF are not over-optimistic.

4.4 Impact on fan design

It was documented in Sects. 4.1 and 4.2 that variable-geometry systems substantially improve the aerodynamic-stability margin of low-pressure fan stages, which is of course their primary objective. As they ensure a safer operation at off-design conditions, their implementation may in turn affect how the fan stage is designed from the beginning. In particular, a part of the gain in stability margin may be translated into designing an aerodynamically more challenging fan rotor with increased loading and reduced blade surface.

This question is addressed in the present section by considering a variation of the rotor blade solidity, defined as the ratio of chord length to blade spacing in circumferential direction. On the one hand, decreasing the solidity makes the fan aerodynamically less stable, but on the other hand, it reduces the fraction of the duct cross-section area occupied by the rotor wakes, as these scale with the rotor overall blade surface. The variation in solidity can be realized either by a change in blade count or in blade chord length.

Figure 20 illustrates three examples of fan designs with different rotor blade chord length, scaled by $\pm 25\%$ of the reference chord length of the SIAM UHBR design. The axial gap between rotor and stator is kept constant, like all other geometry parameters defining the fan stage. The aerodynamic maps calculated for each of these three configurations reveal in Fig. 21 that a reduction in chord length decreases as expected the slope of the iso-speed lines toward surge

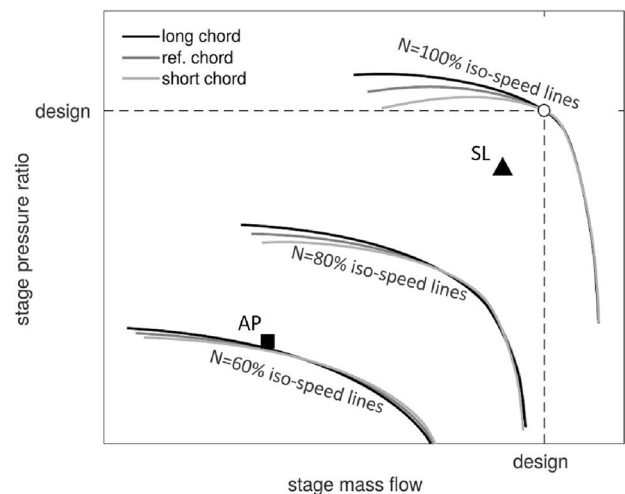


Fig. 21 Aerodynamic performance map of fans with varying rotor chord length

and also decreases the maximum pressure ratio that can be achieved at a given iso-speed line. Hence, the stability margin of the fan at the depicted acoustic points AP and SL is reduced, but this margin may still be sufficiently large with a VAN or VPF system, provided the points have been shifted away from the surge region as described in the previous sections of the paper. For example, a reduction in surge margin from 23 to 20% is estimated at SL between the reference chord length and the short chord decreased by 25%, at optimal nozzle setting of the VAN, which is still well above the value of 14% achieved without any VAN or VPF.

The benefit in fan aerodynamic performance is visualized in Fig. 22. The color code is similar to that of Fig. 19, with VAN results in blue and VPF results in magenta. The lines refer to the case where the chord length is varied, whereas the symbols depict the variation in blade count. On the left part, we observe a continuous slight reduction of stability margin (here considered at Sideline condition only) when the rotor solidity is decreased (either by shortening the chord

Fig. 20 Side view of the UHBR fan stage with varying rotor chord length

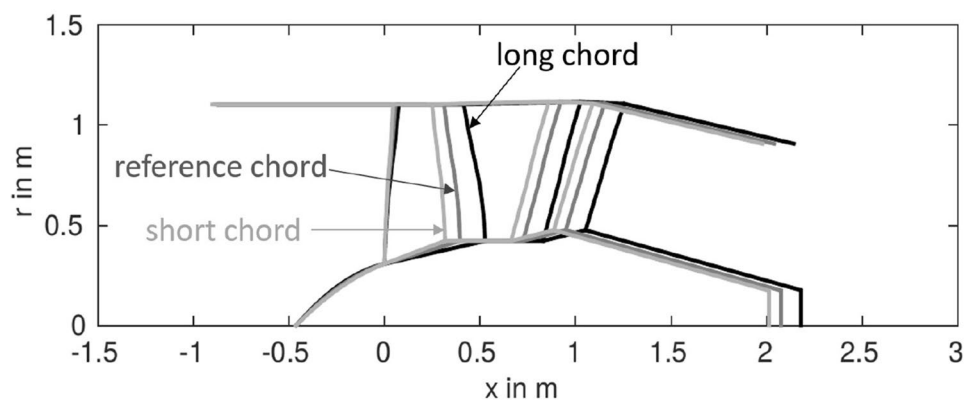
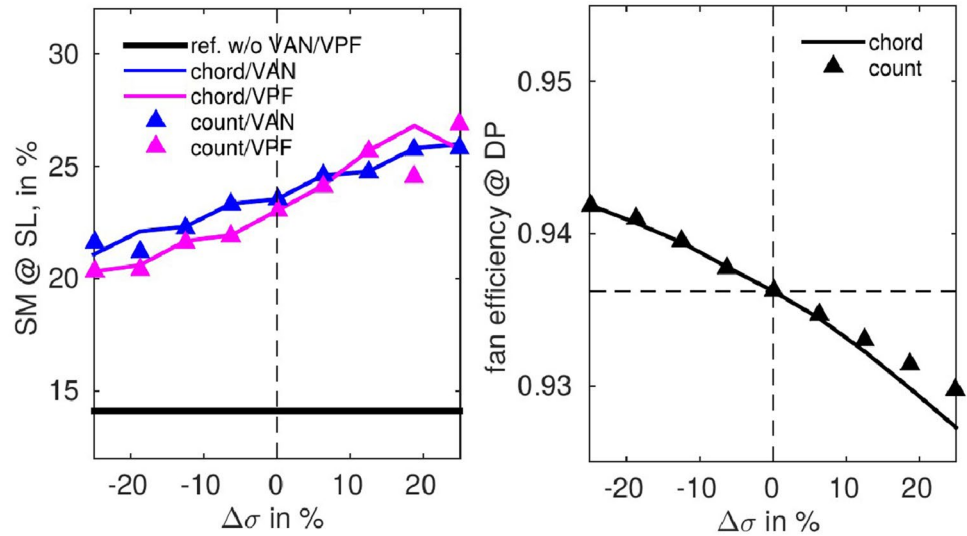


Fig. 22 Impact of a rotor-solidity variation on fan aerodynamic performance: stability margin at SL (left) and isentropic efficiency at DP (right)



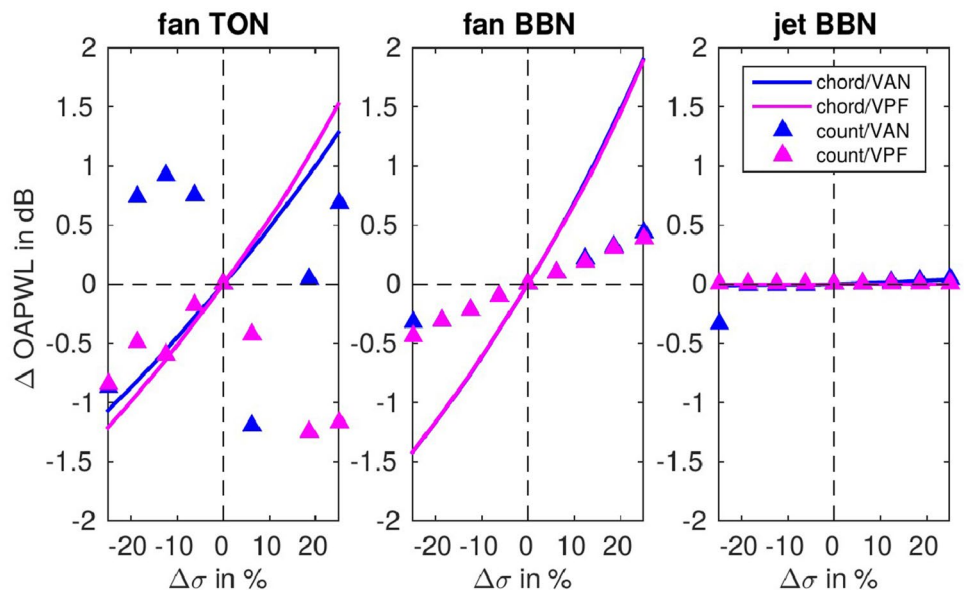
or removing blades); however, even with a 25% solidity cut, the margin remains much higher with the VAN or VPF than in the reference configuration with fixed geometry (black thick line). In addition, the fan efficiency at the design point in Cruise, which strongly drives the fuel consumption of the engine, is continuously improved when decreasing rotor solidity (of course, as long as no massive flow separation occurs); a gain of 0.5% efficiency is achieved with a 25% solidity cut. Hence, it seems meaningful to trade some of the large benefit in stability provided by the VAN and VPF for a lower fuel emission. It is also meaningful from an acoustic perspective, as we develop now.

Figure 23 shows how the engine noise components are affected by a relative change in rotor design solidity at the Sideline acoustic point. First, modifying the rotor design

hardly affects the position of the acoustic points within the map, so jet noise variations are below 0.5 dB and thus very small. Variations in fan broadband noise, however, are much more significant and it turns out that shortening the chord is acoustically more effective than removing blades. Similar conclusions can be made for the fan tonal noise component. The blade chord reduction steadily decreases the tonal noise levels from the rotor, whereas variations in blade count feature a strong scatter of the data. Although not shown, the same trends are observed at Approach conditions.

As a result, it is concluded that the more stable operation at off-design conditions provided by the variable-geometry systems can be leveraged to design more strongly loaded rotor blades. Reducing the blade chord appears to be a more robust and more effective option than removing blades to

Fig. 23 Acoustic impact of a rotor-solidity variation with VAN and VPF systems implemented at optimal setting, and evaluation at SL acoustic point for the three noise components considered



reduce the fan broadband and tonal emission, with a reduction potential near 1.5 dB when the blade chord is reduced by 25% from its reference value. Reducing the chord also results in an axially shorter rotor, which can lead to a more compact engine or an increased distance to the downstream stator, thus reducing further the noise emission from the fan.

5 Conclusion

An acoustic theoretical study has been carried out with an analytical modelling approach that estimates the noise emission of a modern UHBR engine from the jet and from the fan stage. Compared with older designs of engines currently in service, the low-pressure-ratio fan stage shows the expected acoustic benefits in terms of jet noise and fan tonal noise; however, its fan broadband noise levels are not so much competitive with those of the older designs.

The main cause for that is the location inside the aerodynamic fan map of the off-design points relevant for acoustic certification (take-off and approach). Without a variable-geometry system, operation at off-design is too close to the fan surge line, which induces a large positive rotor blade incidence and loading and in turn provokes strong wake and turbulence production and high levels of broadband noise. A variable-geometry system is therefore not only mandatory for aerodynamic-stability reasons but also to allow the modern UHBR designs to maintain a competitive edge over older engines in terms of acoustic emission.

With a variable-area nozzle, that is achieved by opening the nozzle exhaust section and by shifting the location of the off-design points away from the surge line, without affecting the shape of the fan map. The result of that shift is fan operation at larger mass flow and lower pressure ratio, which explains the slight reduction in jet noise by 1–2 dB.

With a variable-pitch fan, closing the rotor blades modifies the shape of the fan aerodynamic map (the constant-speed lines become steeper), but the fan operates at the same pressure ratio and mass flow as in the baseline fixed-geometry configuration, its position being further away from the surge line in the modified fan map. That also explains why jet noise is unaffected by the VPF.

With both technologies, a very substantial fan broadband noise reduction by up to 4 dB is predicted with an aerodynamically optimal VAN opening around 15% at SL and AP conditions, and up to 6 dB with an optimal VPF pitch setting around 5°. This is achieved in both cases by reducing the rotor blade incidence, unloading the fan, and thus preventing the production of large wakes and turbulence. The reduction of fan tonal noise is less obvious with the VAN (below 1.5 dB) but is visible with the VPF (up to 4 dB). It should be mentioned that the good acoustic performance of the VPF may be a bit optimistic, here, as

a practical implementation of that system would require a slightly larger tip clearance at the rotor tip, which may cause a stronger tip vortex and some spurious noise.

Opening the nozzle (in case of the VAN) or closing the rotor (in case of the VPF) beyond the aerodynamic optimum does not provide any additional acoustic benefit in terms of fan noise, because the fan operates then too close from the wind milling region (at AP) or choke region (at SL) and the rotor wakes and flow Mach numbers start to grow again. Moreover, the study suggests that the fan noise reductions achieved with a VPF system are larger than with a VAN, by nearly 2 dB; first, this is attributed to the increased tilting of the rotor wakes and thus increased decay length during their convection toward the stator; a second positive contribution comes from the slightly weaker intra-stage swirl yielding a lower flow Mach number at the OGV entry plane.

By allowing for a more flexible operation of the fan at off-design conditions, the variable-geometry systems may in turn affect how the fan stage is designed. The gain in off-design aerodynamic stability may be traded for a more strongly loaded fan at design Cruise condition, for example by reducing the number of fan rotor blades or by decreasing their chord length. It is shown that shortening the chord is acoustically a more robust and effective measure than removing blades. Gains in fan noise around 1.5 dB are predicted at Take-off Sideline with a reduction in chord by 25%, whereby a gain in Cruise efficiency by 0.5% is observed, while the surge margin still remains 6% above that of the fixed-geometry design. Further acoustic improvements can be realized if the shorter rotor is combined with a longer gap between rotor and stator.

It should be finally mentioned that the conclusions obtained in that study for a transonic/high-subsonic UHBR fan stage are expected to stay applicable for low-speed ducted propulsion systems, but the acoustic benefit from the VAN/VPF might be slightly less significant if the rotor blades are designed with a very large tolerance to off-design incidences.

Acknowledgements This study has been funded by the DLR research project SIAM.

Funding Open Access funding enabled and organized by Projekt DEAL.

Data availability The data corresponding to the results of the study can be made available if requested.

Declarations

Conflict of interest The authors declare that they have no conflicts of interest. The study has involved no animals or humans as subjects.

Open Access This article is licensed under a Creative Commons Attribution 4.0 International License, which permits use, sharing,

adaptation, distribution and reproduction in any medium or format, as long as you give appropriate credit to the original author(s) and the source, provide a link to the Creative Commons licence, and indicate if changes were made. The images or other third party material in this article are included in the article's Creative Commons licence, unless indicated otherwise in a credit line to the material. If material is not included in the article's Creative Commons licence and your intended use is not permitted by statutory regulation or exceeds the permitted use, you will need to obtain permission directly from the copyright holder. To view a copy of this licence, visit <http://creativecommons.org/licenses/by/4.0/>.

References

- Freeman, C., Cumpsty, N.: Method for the prediction of supersonic compressor blade performance. *J. Propuls.* **8**, 199–208 (1992). <https://doi.org/10.2514/3.23461>
- Giannakakis, P.: Design space exploration and performance modelling of advances turbofan and open-rotor engines. PhD Thesis, Cranfield University, UK (2013)
- Ginder, R., Newby, D.: A study of factors affecting the broadband noise of high-speed fans. In: AIAA 3rd Aeroacoustic Conference, AIAA 1976-567, Palo Alto (1976). <https://doi.org/10.2514/6.1976-567>
- Glaser, F., Woodward, R., Lucas J.: Acoustic and aerodynamic performance of a variable-pitch 6-ft.-diameter 1.2-pressure-ratio fan stage (QF-9). NASA Technical Note D-8042 (1977)
- Joksimovic, A., Duplaa, S., and Bousquet, Y., Carbonneau, X., Tantot, N.: Local and global analysis of a variable-pitch-fan turbofan engine. In: Proceedings of the 12th European Conference on Turbomachinery Fluid Dynamics and Thermodynamics, Stockholm, Sweden, Paper ETC-2017-073 (2017). <https://doi.org/10.29008/ETC2017-073>
- Kaplan, B.: Design of an advanced fan stage with ultra high bypass ratio and comparison with experimental results. PhD Thesis, Ruhr-University of Bochum (2010)
- Kavvalos, M., Zhao, X., Schnell, R., Aslanidou, I., Kalfas, A., Kyprianidis, K.: A modelling approach of variable geometry for low-pressure-ratio fans. In: Proceedings of the ISABE Conference, Paper ISABE-2019-24382 (2019)
- Krejsa, E., Stone, J.: Enhanced fan noise modelling for turbofan engines. NASA Contractor Report 2014-218421 (2014)
- Kyritsis, V.: Thermodynamic preliminary design of civil turbofans and variable-geometry implementation. PhD thesis, Cranfield University, UK (2006)
- Lown, H.: Aeroacoustic experimental verification of optimum configuration of variable-pitch fans for 40x80 foot subsonic wind tunnel. NASA Contractor Report CR-152040 (1977)
- Meier zu Ummeln, R., Moreau, A.: Enhanced prediction of fan broadband noise with improved aerodynamic models in Prop-Noise. Final report for Clean Sky 2 EU project ADEC, Deliverable D1.1.14-14 (2022)
- Mennicken, M.: Electrically powered engine simulator: a technology demonstrator. Work package 1–88.2-inch full-scale fan stage. Project report (2021)
- Michel, U.: The benefits of variable-area fan nozzle on turbofan engines. In: Proceedings of the 49th AIAA Aerospace Sciences Meeting Including the New Horizons Forum and Aerospace Exposition, Orlando, Florida, Paper AIAA-2011-0226 (2011). <https://doi.org/10.2514/6.2011-226>
- Moreau, A.: A unified analytical approach for the acoustic conceptual design of fans of modern aero-engines. PhD Thesis, Technical University of Berlin (2017). <https://doi.org/10.14279/depositonnce-5935>
- Moreau, A., Guérin, S.: Experimental validation of an analytical prediction model for fan buzz-saw noise. In: Proceedings of the ASME Turbo Expo Conference, paper GT2020-14279 (2020). <https://doi.org/10.1115/GT2020-14279>
- Moreau, A.: Theoretical acoustic benefit of high bypass ratio and variable area nozzle in turbofan engines. In: Proceedings of 14th European Conference on Turbomachinery Fluid Dynamics & Thermodynamics, ETC14, Paper ETC2021-700, Gdansk (2021). <https://doi.org/10.29008/ETC2021-700>
- Sain, C., Hoeschler, K., Mischke, M.: Concept study of variable-area fan nozzle for ultra-high bypass ratio. In: Proceedings of the ISABE Conference, Paper ISABE-2015-22165 (2015)
- Schoenweitz, D., Becker, R.-G., Schnell, R., Schroll, M.: Aerodynamic performance characteristics of the installed V2527 fan at ground operation. In: Proceedings of the 54th AIAA Aerospace Sciences Meeting, Paper AIAA 2016-0111, San Diego (2016). <https://doi.org/10.2514/6.2016-0111>
- Schnell, R., Goldhahn, E., Julian, M.: Design and performance of a low-fan-pressure-ratio propulsion system. In: Proceedings of the 2th Conference of the International Society for Air Breathing Engines ISABE Conference. Paper ISABE-2019-24017, Canberra (2019)
- Siller, H., Bassetti, A., Funke, S.: Investigation of turbomachinery and jet noise of the V2500 engine during ground tests with an A320 aircraft. In: 11th European Turbomachinery Conference, 23–27. March 2015, Madrid, Spain (2015)
- Stone, J., Groesbeck, D., Zola, C.: Conventional profile coaxial jet noise prediction. *AIAA J.* **21**, 336–342 (1983). <https://doi.org/10.2514/3.8077>
- Williams, T., Hall, C.: Reverse thrust aerodynamics of variable pitch fans. In: Proceedings of ASME Turbo Expo 2018, Oslo, Paper GT2018-75739 (2018). <https://doi.org/10.1115/1.4043139>
- Woodward, R., Hughes, C.: Noise benefits of increased fan bypass nozzle area. In: NASA Technical Memorandum TM-2004-213396 (2004) (also Published as Conference Paper AIAA-2005-1201). <https://doi.org/10.2514/6.2005-1201>

Publisher's Note Springer Nature remains neutral with regard to jurisdictional claims in published maps and institutional affiliations.